

Operating Characteristics of Heavy Loaded Cylindrical Journal Bearing with Variable Axial Profile

Stanislaw Strzelecki*

Lodz University of Technology, Department of Mechanical Engineering,
90-924 LODZ, Poland, Stefanowskiego 1/15

Received: July 19, 2004; Revised: July 25, 2005

During the operation of turbounit its bearings displace as a result of heat elongation of bearings supports. It changes the static deflection line of rotor determined during assembly of the turbounit, causing an increase in the stresses on the bearing edges and a decrease in the dynamic state of the machine. One of possibilities to avoid the edge stresses is to apply the bearings with variable axial profile, e.g. hyperboloidal, convex profile in the axial cross-section of bearing. Application of journal bearings with hyperboloidal profile allows to extend the bearing operation range without the stress concentration on the edges of bush. These bearings successfully carry the extreme load in conditions of misaligned axis of journal and the bush eliminating the necessity of using self-aligning bearings. Operating characteristics of bearing include the resulting force, attitude angle, oil film pressure and temperature distributions, minimum oil film thickness, maximum oil film temperature. In literature there is a lack of data on the operating characteristics of heavy loaded hyperboloidal journal bearings operating at the conditions of adiabatic oil film and static equilibrium position of the journal. For the hyperboloidal bearing the operating characteristics have been obtained. Different values of length to diameter ratio, assumed shape and inclination ratio coefficients have been assumed. Iterative solution of the Reynolds', energy and viscosity equations was applied. Adiabatic oil film, laminar flow in the bearing gap as well as aligned and misaligned orientation of journal in the bush were considered.

Keywords: lubrication, journal bearings

1. Introduction

The fulfilment of condition for journal and bush axis parallelism as well as co-axiality of bushes bores, is problematic in the practice. An increase in precise positioning of these elements causes a significant increase in costs of machining.

The rotor which is generally supported between two bearings (Figure 1a) causes bending of shaft in relation to the bearing. Misaligned shaft affects the bearings characteristics and significantly diminishes the range of safe bearing operation. It generates the mixed friction and transient conditions of unstable operation. Misalignment of journal bearing can be caused by position errors, too (Figure 1b).

Journal bearings with hyperboloidal profile extend the bearing operation range without the stress concentration on the edges of bush. The load can be carried without application of self-aligning bearings, Burcan¹.

High speed bearings are slightly loaded opposite to the low speed heavy loaded ones. Romacker² defines slightly loaded bearings as the bearings running at relative eccentricities of journal smaller than 20%, at Sommerfeld numbers about 0.1 for the bearings with the length to diameter ratio 0.5. Operating characteristics of these bearings can be determined by means of one dimensional energy equation. Heavy loaded bearings have to be calculated by means of the two or three dimensional energy equation. Calculation procedure should deliver the temperature in each point within oil film. Assumption of mean temperature on the oil film thickness accelerates the calculation.

In literature, there is a lack of data on the operating characteristics of heavy loaded misaligned hyperboloidal journal bearings running with laminar, adiabatic oil film and at the static equilibrium position of the journal.

For the hyperboloidal bearing the operating characteristics as oil film pressure, temperature fields, static equilibrium position

angle, Sommerfeld number, maximum oil film temperature have been obtained by iterative solution of the Reynolds', energy and viscosity equations. Adiabatic oil film, laminar flow in the bearing gap as well as aligned and misaligned orientation of journal in the bush, were considered. Static equilibrium position of the journal³⁻⁵ was assumed too.

2. Geometry of Lubricating Gap

The profile variation of hyperboloidal bearing which is given by Equation 1 gives in reality a negligible modification of cylindrical bush; it allows to use the Reynolds Equation 2 for describing the oil flow in the bearing gap, Burcan¹. The case of misaligned axis of journal and bush of hyperboloidal profile is showed in Figure 2. The oil film thickness is given by the following equation:

$$\bar{H} = 1 + \varepsilon \cos(\varphi - \alpha) + c\bar{z}^2 + q\bar{z} \cos(\varphi - \alpha) \quad (1)$$

Since the hyperboloidal bearing has larger side oil leakages and the loss of load capacity is larger than for the cylindrical one, the bearing profile coefficient c should not exceed 0.3 (Figure 3). Boundary values of relative eccentricity are in Figure 4.

3. Oil Film Pressure and Temperature Distribution

Pressure distribution has been defined from Equation 2 on the assumption of variable viscosity

$$\frac{\partial}{\partial \varphi} \left(\frac{\bar{H}^3}{\eta} \frac{\partial \bar{p}}{\partial \varphi} \right) + \left(\frac{D}{L} \right)^2 \frac{\partial}{\partial z} \left(\frac{\bar{H}^3}{\eta} \frac{\partial \bar{p}}{\partial z} \right) = 6 \frac{\partial \bar{H}}{\partial \varphi} + 12 \frac{\partial \bar{H}}{\partial \varphi} \quad (2)$$

It has been assumed for the pressure region that the oil is supplied under pressure p_{supp} into the grooves, on the bearing edges

*e-mail: strzelec@pkm1.p.lodz.pl

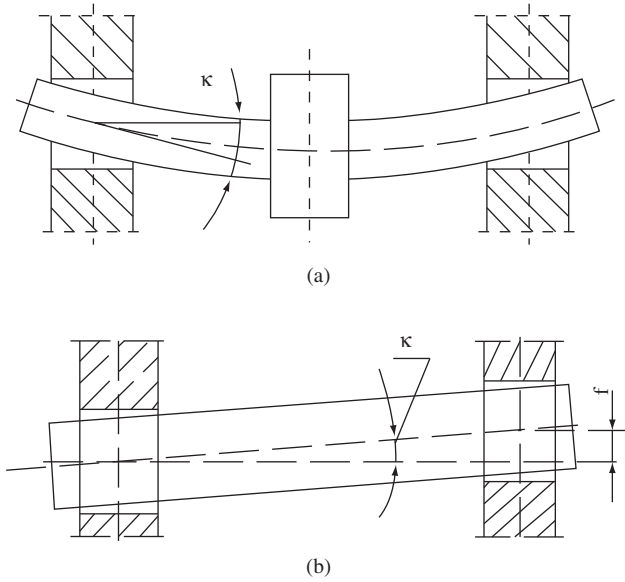


Figure 1. a) Bending of the shaft; and b) position errors at stiff shaft.

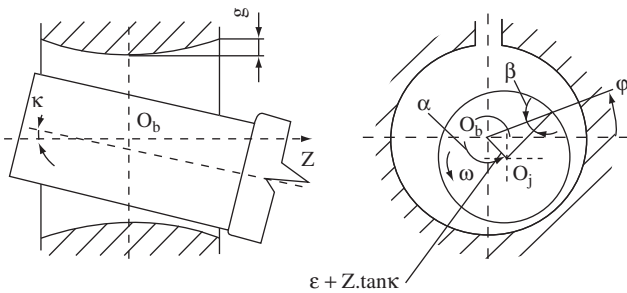


Figure 2. Geometry of hyperboloidal bearing.

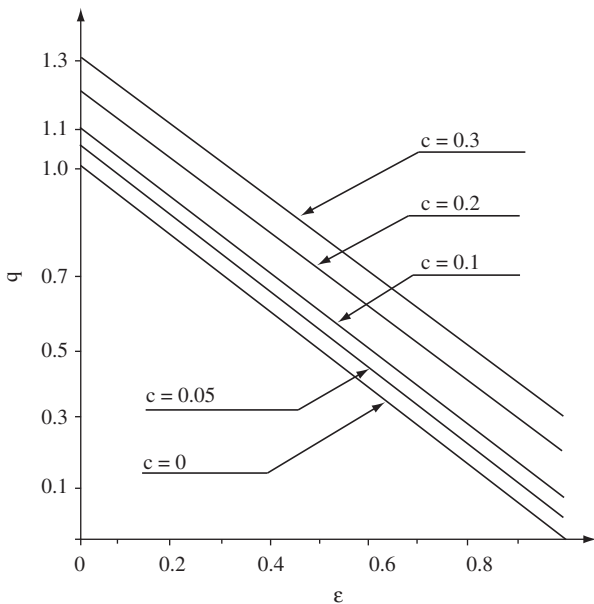


Figure 3. Relative inclination ratio q vs. the bearing relative eccentricity ε for different values of hyperboloidal profile coefficient c, Burcan¹.

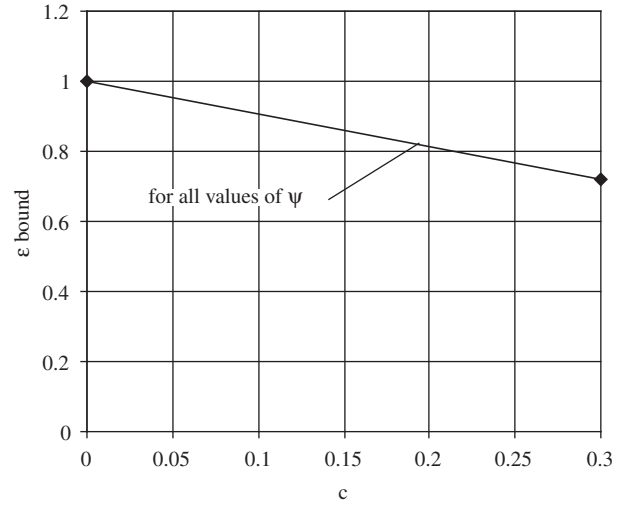


Figure 4. Boundary values of relative eccentricity (in the middle plain of bush) over hyperboloidal profile coefficient c Burcan¹.

(z = ± L/2) the oil film pressure p(φ, z) = 0, and in the regions of negative pressures, p(φ, z) = 0.

Oil film pressure distribution computed from Equation 2 has been put in the transformed energy Equation 3.

$$\frac{\bar{H}}{Pe} \left[\frac{\partial^2 \bar{T}}{\partial \varphi^2} + \left(\frac{D}{L} \right)^2 \frac{\partial^2 \bar{T}}{\partial z^2} \right] + \left[\frac{\bar{H}^3}{12\bar{\eta}} \frac{\partial \bar{p}}{\partial \varphi} - \frac{\bar{H}}{2} \right] \frac{\partial \bar{T}}{\partial \varphi} + \left(\frac{D}{L} \right)^2 \frac{\bar{H}^3}{12\bar{\eta}} \frac{\partial \bar{p}}{\partial z} \frac{\partial \bar{T}}{\partial z} = - \frac{\bar{H}^3}{12\bar{\eta}} \left[\left(\frac{\partial \bar{p}}{\partial \varphi} \right)^2 + \left(\frac{D}{L} \right)^2 \left(\frac{\partial \bar{p}}{\partial z} \right)^2 \right] - \frac{\bar{\eta}}{\bar{H}} \quad (3)$$

The viscosity is described by exponential equation^{3,5}. Temperature and viscosity distribution has been found by the iterative solution of Equations 1, 2 and 3³. The boundary condition for the temperature takes into account the temperature of inlet oil. Temperature values T(φ, z) on the boundaries (z = + L / 2) have been determined by means of the parabolic approximation³.

4. Results of Calculation

Numerical calculations were performed for two different values of aspect ratio i.e. L/D = 0.5 and 1.0, clearance ratio ψ = 1.5‰, hyperboloidal profile coefficient c = 0.0, 0.05, 0.1, 0.2 and relative inclination ratio q = 0.0 and 0.1.

These sets of parameters allow to determine the effect of:

- Bush geometry i.e. bearing length to diameter ratio L/D and shape coefficient c;
- Journal position i.e. relative inclination ratio q and relative eccentricity on the operating characteristics which include the oil film: pressure \bar{p} , temperature \bar{T} distributions, Sommerfeld number So, static equilibrium position angle α_{eq} , oil film thickness \bar{H} and maximum temperature \bar{T}_{max} ;
- Some results of calculations have been presented for the relative eccentricity ε = 0.6 corresponding to the conditions of heavy loaded bearing.

Results of theoretical calculation have been presented in Figure 5 through Figure 18. Computed oil film thickness \bar{H} in the axial cross-section of bearing and for different values of hyperboloid profile coefficient c, can be seen in Figure 5. Sommerfeld numbers So obtained at different hyperboloid profile coefficients c and relative inclination

coefficient q are shown in Figure 6; at assumed hyperboloid profile coefficient c an increase in relative inclination coefficient q causes the increase in Sommerfeld number and the values are smaller in case of hyperboloid bearing ($c \neq 0$). Than in case of cylindrical one ($c = 0$). Static equilibrium position angles α_{eq} obtained for two values of bearing length to diameter ratio L/D and assumed values of hyperboloid profile coefficient, are given in Figure 7; there is a small decrease in static equilibrium position angles α_{eq} with an increase in hyperboloid profile coefficient c . Maximum oil film temperature T_{max} computed at different hyperboloid profile coefficients c are shown in Figure 8; an increase in profile coefficient c causes the increase in maximum oil film temperature.

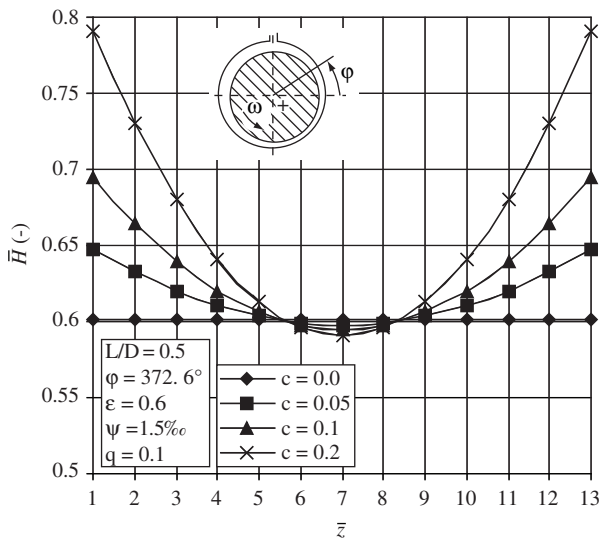


Figure 5. Oil film thickness in the axial cross section at the chosen angular coordinate and for different hyperboloid coefficients.

Oil film pressure and temperature distributions for the bearing with the length to diameter ratio $L/D = 1.0$ relative eccentricity $\epsilon = 0.6$ and hyperboloid profile coefficient $c = 0.2$ are shown in Figure 9 and Figure 10, these distributions are for axial coordinate ranging from $\bar{z} = 1$ and $\bar{z} = 7$. An effect of hyperboloidal profile coefficient c on the oil film pressure and temperature distributions in the peripheral and axial directions can be observed in Figure 11 through Figure 18. In the range of assumed values, the hyperboloid profile coefficient c has little effect on both distributions (Figure 11 and Figure 12); oil film pressure distribution shows the decrease in the neighbourhood of peak pressures (Figure 11). Comparison of the oil film pressure and temperature distributions for two values of

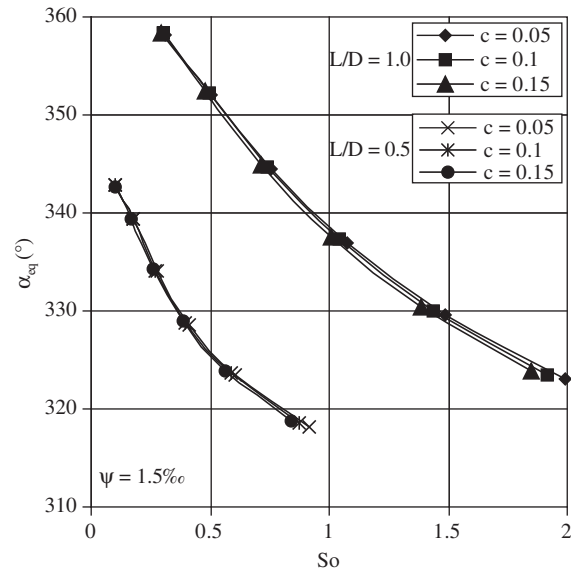


Figure 7. Static equilibrium position angle for different bearing length to diameter ratio and hyperboloid shape coefficient.

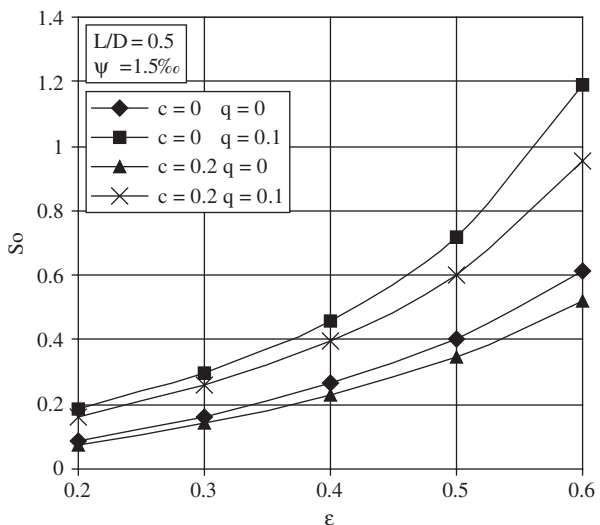


Figure 6. Effect of hyperboloid coefficient c and relative inclination ratio q on the Sommerfeld number.

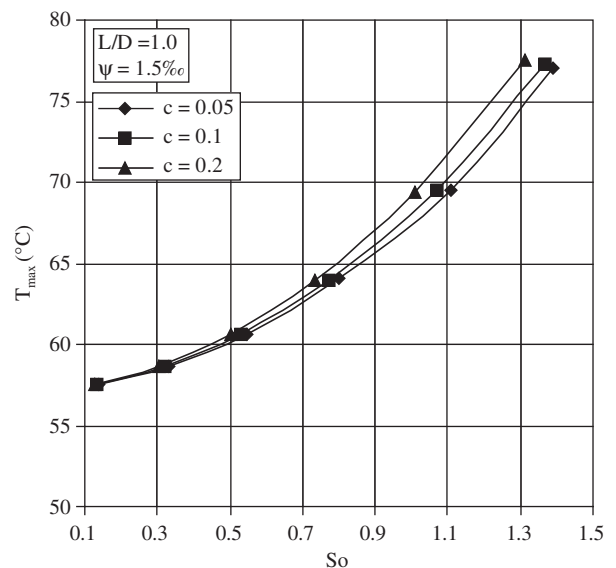


Figure 8. Maximum oil film temperature for different hyperboloid profile coefficient.

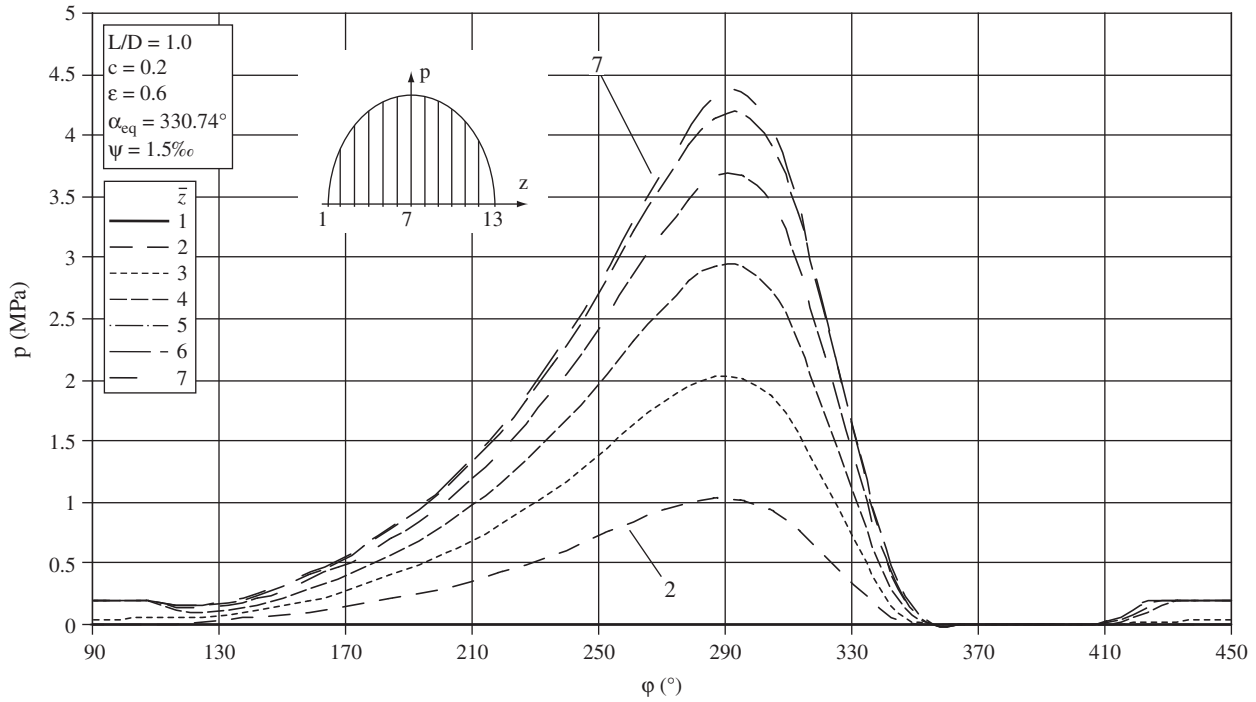


Figure 9. Oil film pressure distributions in different peripheral cross-sections of bearing.

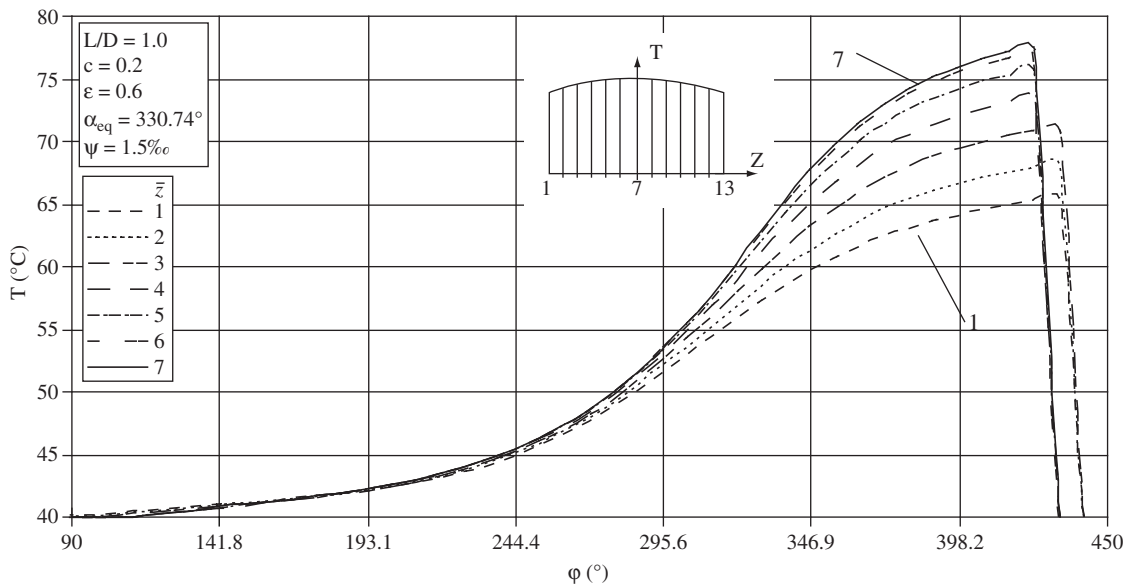


Figure 10. Oil film temperature distributions in different peripheral cross-sections of bearing.

bearing length to diameter ratio L/D at assumed hyperboloid profile coefficient c , shows larger changes of oil film pressures (Figure 13) than the temperatures (Figure 14).

The oil film pressure and temperature distributions calculated in axial cross-sections of bearing at different peripheral coordinates ϕ and different hyperboloidal profile coefficients c are shown in Figure 15 and Figure 16; there is a decrease in the values of pressure

(Figure 15) and in the side temperatures (Figure 16) at the increase in the values of hyperboloid profile coefficient c .

An effect of relative inclination ratio q on the oil film temperature distribution in the axial cross-sections, at different values of hyperboloid profile coefficient c and at assumed peripheral coordinate ϕ , can be observed in Figure 17 and Figure 18. An increase in hyperboloid profile coefficient c causes the strong decrease in the values of temperature on the sides of bearing.

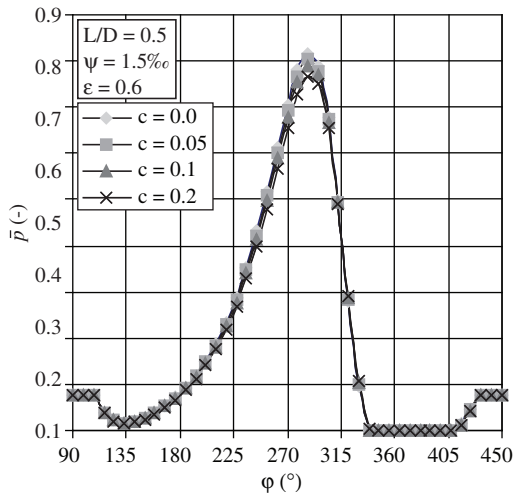


Figure 11 Oil film pressure distribution for different values of hyperboloid profile coefficient.

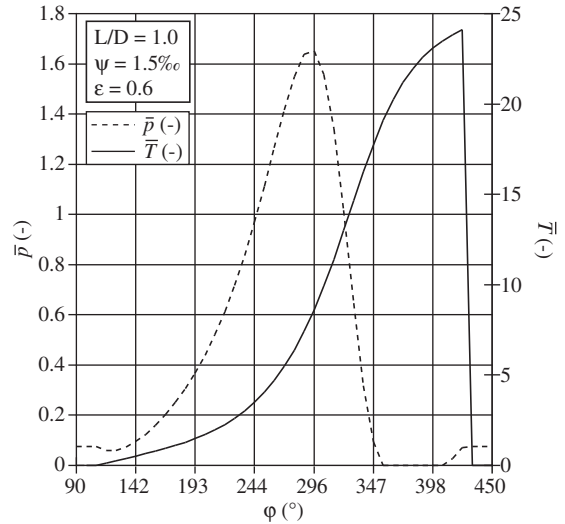


Figure 14 Oil film pressure and temperature distributions at assumed relative eccentricity.

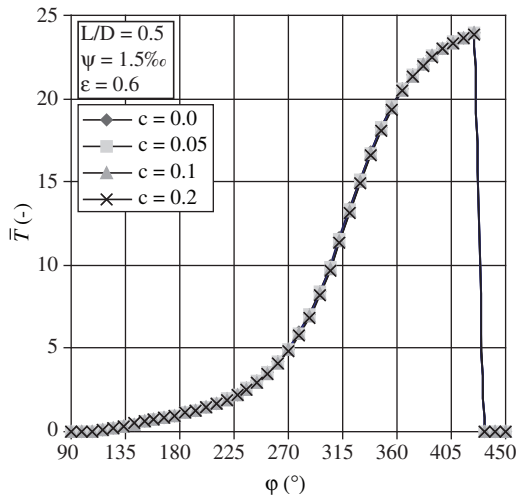


Figure 12 Oil film temperature distribution for different values of hyperboloid profile coefficient.

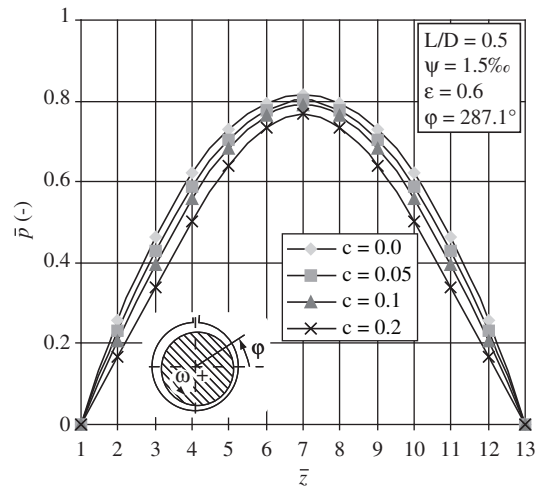


Figure 15 Oil film pressure distributions at assumed relative eccentricity.

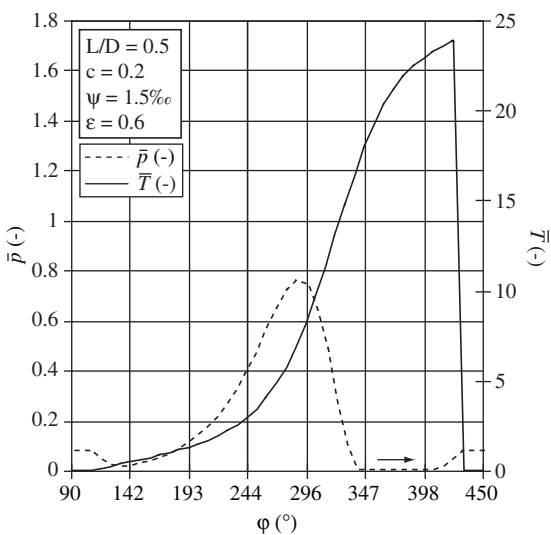


Figure 13 Oil film pressure and temperature distributions at assumed relative eccentricity.

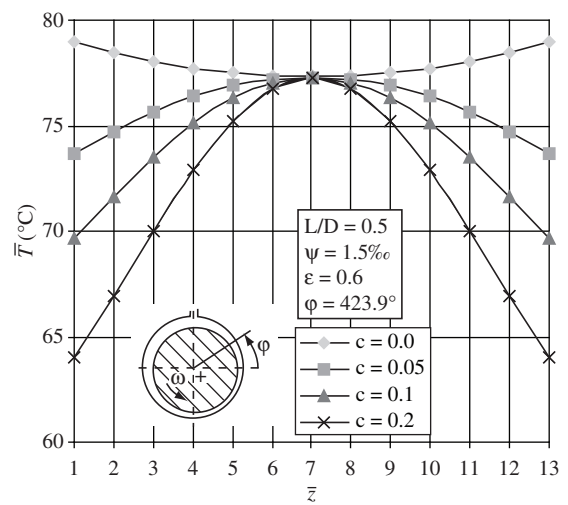


Figure 16 Oil film temperature distributions at assumed relative eccentricity.

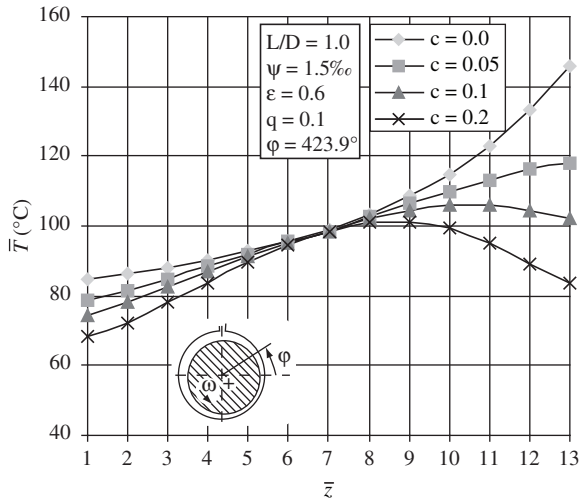


Figure 17. Oil film temperature distribution at assumed relative eccentricity.

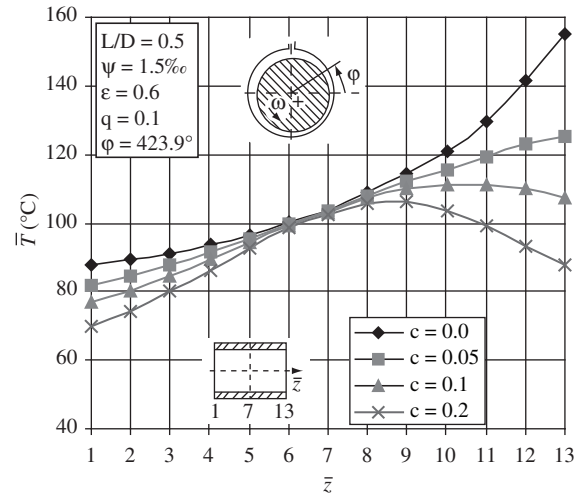


Figure 18. Oil film temperature distributions at assumed relative eccentricity.

5. Conclusions

The results of calculation of operating characteristics of aligned and misaligned, hyperboloidal journal bearing have been presented. They allow the following conclusions:

1. Developed program of computation allows theoretical investigation of aligned and misaligned journal bearings with hyperboloid profile of the bush;
2. The oil film pressure and temperature distributions in the axial direction are influenced by the hyperboloid profile coefficient and relative inclination one;
3. The maximum oil film temperature shows small increase with the increase in the hyperboloidal profile coefficient at assumed load capacity and assumed length to diameter ratio.

References

1. Burcan J. Hyperboloidal journal bearing. 1973. *Problems of Machine Exploitation*; 1973. p. 321-333.
2. Romacker B. *Die Temperaturverteilung im Schmierfilm konstant belasteter Gleitlager. Technische Untersuchungen und Entwicklung eines Messverfahrens.* [D.Phil.thesis]. Karlsruhe. University of Technology Karlsruhe; 1965.
3. Strzelecki S. Operating conditions of hyperboloidal journal bearing with nonisothermal oil film. In: Stachowiak G, editor. *AUSTRIB'94, Frontiers in Tribology Proceedings of the 4th International Tribology Conference. 1994 Dec 5-8; Perth, Australia.* Perth: Perth University. 1994. p. 579-585.
4. Strzelecki S, Litwicki W. Static characteristics of 2-lobe hyperboloidal journal bearing. In: Burcan J, editor. *Non-Conventional Bearings Systems. Proceedings of the 3rd Conference on the Problems of Non-Conventional Bearings Systems. 1997 Aug 12-16, Lodz, Poland.* Lodz: Lodz University of Technology. 1997. p. 125-132.
5. Strzelecki S, Litwicki W. Dynamic characteristics of hyperboloidal 2-lobe journal bearing. In: Institute of Fluid Flow Machinery, editor. *Modelling and Design in Fluid-Flow Machinery. Proceedings of the IMP'97 Conference. 1997 June 12-16, Gdansk, Poland.* Gdansk, Institute of Fluid Flow Machinery. 1997. p. 339-344.

Nomenclature

- c hyperboloidal profile coefficients
 D bush diameter (m)
 F_{stat} static load of the bearing (N)
 g value of hyperboloidal bush modification in relation to cylindrical one measured on the bush face (m)
 h oil film thickness (m)
 \bar{H} dimensionless oil film thickness $\bar{H} = h/(R-r)$
 L bearing length (m)
 p oil film pressure (MPa)
 \bar{p} dimensionless pressure, $\bar{p} = p \cdot \psi^2 / (\eta \cdot \omega)$
 Pe Peclet's number $\rho c \omega r^2 / h$
 q inclination ratio, $q = (L/s) \cdot \tan \kappa$
 r journal diameter (m)
 R bush diameter (m)
 So Sommerfeld number, $So = F_{stat} \cdot \psi^2 / (L \cdot D \cdot \eta \cdot \omega)$
 \bar{T} dimensionless temperature, $\bar{T} = T/T_0$
 T Temperature, (°C)
 T_0 supplied oil temperature (°C)
 t time (s)
 \bar{z} dimensionless axial coordinate, $\bar{z} = 2z/L$
 α attitude angle (°)
 $\bar{\eta}$ dimensionless viscosity, $\bar{\eta} = \eta/\eta_0$
 η dynamic viscosity (Ns/m²)
 η_0 dynamic viscosity at ambient temperature (Ns/m²)
 α_{eq} attitude angle in static equilibrium position of the journal (°)
 ϕ circumferential coordinate (°)
 ϕ dimensionless time, $\phi = \omega t$
 κ inclination angle in the middle plane of bearing (longitudinal cross section)
 ϵ relative eccentricity, $\epsilon = e / (R - r)$
 ψ relative bearing clearance, $\psi = s/D$ (‰)
 ω angular velocity, s⁻¹
 ‰ per mil (‰ = 10⁻³)